



## Abstract

Low resolution and lack of chronostratigraphic calibration of carbonate platform biostratigraphy hinder precise correlation with coeval deep-water successions. This is the main obstacle when studying the record of Mesozoic oceanic anoxic events in carbonate platforms. In this paper we use carbon isotope stratigraphy to produce the first chronostratigraphic calibration of the Barremian–Aptian biostratigraphy of the Apenninic carbonate platform of southern Italy. According to our calibration, the “Selli level” black shales of epicontinental and oceanic basins corresponds in the southern Apenninic carbonate platform to the interval between the “Orbitolina level”, characterized by the association of *Mesorbitolina parva* and *Mesorbitolina texana*, and the second acme of *Salpingoporella dinarica*. The biocalcification crisis of nannoconids corresponds to the interval going from the first acme of *S. dinarica* to just above the top of the “Orbitolina level”. Since these bioevents have been widely recognized beyond the Apenninic platform, our calibration can be used to pinpoint the interval corresponding to the Early Aptian oceanic anoxic event in other carbonate platforms of central and southern Tethys.

## 1 Introduction

The Early Aptian oceanic anoxic event 1a (OAE1a), also known as the Selli event, was a time of severe perturbation of the global carbon cycle. The most popular scenario holds that intense volcanism, associated with the emplacement of the Ontong-Java large igneous province, forced the rapid increase of atmospheric  $p\text{CO}_2$  which triggered a cascade of palaeoenvironmental changes (Larson and Erba, 1999; Méhay et al., 2009; Tejada et al., 2009). The deposition on a global scale of organic-rich marine sediments, the demise of many carbonate platforms at the northern margin of the Tethyan ocean and a biocalcification crisis recorded by calcareous nannoplankton, are among the most significant testimonies left in the geological record (Arthur et al., 1990; Wissler et al., 2003; Weissert and Erba, 2004; Erba et al., 2010).

Most of what we know about the response of the Earth System to the perturbations

SED

3, 789–838, 2011

## Bio-chemostratigraphy of the Barremian-Aptian shallow-water

M. Di Lucia et al.

Title Page

Abstract

Introduction

Conclusions

References

Tables

Figures

⏪

⏩

◀

▶

Back

Close

Full Screen / Esc

Printer-friendly Version

Interactive Discussion





---

**Bio-  
chemostratigraphy of  
the Barremian-Aptian  
shallow-water**M. Di Lucia et al.

---

[Title Page](#)[Abstract](#)[Introduction](#)[Conclusions](#)[References](#)[Tables](#)[Figures](#)[Back](#)[Close](#)[Full Screen / Esc](#)[Printer-friendly Version](#)[Interactive Discussion](#)

The chronostratigraphic scale tied to these shallow water biostratigraphic schemes conveys the impression that long-distance precise correlation between different carbonate platforms, as well as correlation with coeval deep-water facies, can be easily attained. However, a more in-depth appraisal of the papers on the biostratigraphy of Tethyan carbonate platforms reveals that the chronostratigraphic calibration of the biozones is admittedly tentative (De Castro, 1991; Chiocchini et al., 2008) or entirely based on the age of orbitolinid foraminifera as established in the Urgonian Platforms of the Northern Tethyan margin (Bachmann and Hirsch, 2006; Velić, 2007).

In the absence of black shales and of a reliable biostratigraphic criterion, the identification of segments corresponding to the Selli event in the resilient carbonate platforms of the central and southern Tethys is generally based on carbon isotope stratigraphy. However, the pristine carbon isotope signal of the open ocean can be modified by local palaeoceanographic processes and later overprinted to a considerable extent by diagenesis (see Immenhauser et al., 2008, for a recent review). As a result, many published carbon isotope profiles of Lower Cretaceous shallow-water carbonate successions are markedly different from, and very difficult to correlate with, basinal reference curves (D'Argenio et al., 2004; Huck et al., 2010; Tešović et al., 2011).

In this paper we present the carbon isotope stratigraphy and biostratigraphy of three Barremian–Aptian successions of the Apenninic carbonate platform of southern Italy. By correlating the carbon isotope profiles of the studied successions to well dated reference curves of basinal successions, we obtain a chronostratigraphic calibration for some widely used shallow-water biostratigraphic events. The most significant result of our study is the proposal of chemostratigraphically constrained biostratigraphic criteria for the individuation of the time-equivalent of the Selli event and of the Barremian–Aptian boundary in central and southern Tethyan carbonate platforms.

## 2 Geological setting

The shallow-water carbonates that are widely exposed in southern Italy (Fig. 2) are the relics of carbonate banks that developed during the Mesozoic on the passive margin of Adria, a promontory of the African Plate (Bosellini, 2002). Starting from the Middle Triassic, the continental rifting individuated two wide platforms, the Apenninic platform and the Apulian platform, separated by a deep basin (the Lagonegro Basin). Shallow-water carbonate sedimentation persisted almost to the end of the Cretaceous, when the platforms emerged, and was locally re-established during the Palaeogene and the Early Miocene to be eventually terminated by drowning and siliciclastic deep-water deposits. The total thickness of the Mesozoic succession of the Apenninic carbonate platform can be estimated to about 4–5 km with about 1–1.2 km pertaining to the Cretaceous (Sartoni and Crescenti, 1962; D'Argenio and Alvarez, 1980; Frijia et al., 2005). The Upper Triassic to Lower Cretaceous limestones and dolomites are generally referred to flat-topped, Bahamian-type tropical carbonate platforms, dominated by chloralgal and chlorozoan associations (D'Argenio et al., 1975) whereas the depositional system of the Upper Cretaceous rudist limestones has been interpreted as a ramp-like open shelf, dominated by foramol-type assemblages (Carannante et al., 1997).

## 3 Materials and methods

### 3.1 Sedimentology and biostratigraphy

Three shallow-water carbonate successions have been selected for this study: Mt. Croce (north of Formia, Lazio), Mt. Motola (south of Salerno, Campania) and Mt. Coccovello (north of Maratea, Basilicata) (Fig. 2).

The studied sections have been logged in the field at decimetre to meter scale, depending on the outcrop quality, and sampled with an average resolution of about one

SED

3, 789–838, 2011

## Bio- chemostratigraphy of the Barremian-Aptian shallow-water

M. Di Lucia et al.

Title Page

Abstract

Introduction

Conclusions

References

Tables

Figures

⏪

⏩

◀

▶

Back

Close

Full Screen / Esc

Printer-friendly Version

Interactive Discussion





hand lens. The samples were then passed through a complete procedure of diagenetic screening, involving standard petrography (optical microscopy, cathodoluminescence and SEM) and analysis of minor and trace element concentration (see Friija and Par-  
5 ente, 2008, for a full description of the screening procedure and for analytical details).

The numerical ages of the samples were derived from the look-up table of McArthur  
et al. (2001, version 4: 08/04), which is tied to the GTS2004. Minimum and maximum  
ages were obtained by combining the statistical uncertainty (2 s.e.) of the mean values  
of the Sr-isotope ratios of the samples with the uncertainty of the seawater curve.

## 4 Results

### 4.1 Lithostratigraphy, lithofacies associations and palaeoenvironmental 10 interpretation

From a lithostratigraphic point of view the three studied sections belong entirely to  
the “Calcarei con Requenie e Gasteropodi” formation (Requenie and Gastropod lime-  
stones Fm). Eight Lithofacies Associations (LA) (Table 1) have been identified on the  
15 basis of texture, components (with special emphasis on fossil assemblages) and sedi-  
mentary structures. The main skeletal components are mollusks (gastropods, ostreids  
and requenieid rudists), benthic foraminifers and green algae, with additional contribu-  
tion from microbial nodules and crusts. Non-skeletal grains are mainly represented  
by peloids and intraclasts. The nomenclature of the LA conforms to that adopted by  
20 previous Authors for the Lower Cretaceous carbonates of the Apenninic carbonate plat-  
form and of other carbonate platforms of the central-southern Tethyan domain (Raspini,  
2001; Pittet et al., 2002; Hillgärtner et al., 2003; D’Argenio et al., 2004; Bachmann and  
Hirsch, 2006). The described lithofacies represent a full range of sub-environments,  
from supratidal marsh with ponds, to tidal flat to subtidal restricted to open lagoon  
25 (Fig. 3). A synoptic description of LA is given in Table 1. All the studied successions  
can be generally referred to an inner platform setting. The Monte Croce section shows

## Bio- chemostratigraphy of the Barremian-Aptian shallow-water

M. Di Lucia et al.

Title Page

Abstract

Introduction

Conclusions

References

Tables

Figures



Back

Close

Full Screen / Esc

Printer-friendly Version

Interactive Discussion



more open marine facies, organized mainly in subtidal and, subordinately, in peritidal metric cycles. More restricted environments occur at Mt. Motola and Mt. Coccovello, where peritidal cycles dominate the successions and subaerial exposure surfaces are more prominent and frequent.

## 5 4.2 Biostratigraphy

The following species of benthic foraminifers and calcareous algae have been used in this paper for the biostratigraphic subdivision and correlation of the studied successions (Figs. 4, 5)

- *Praechrysalidina infracretacea* LUPERTO SINNI, 1979
- 10 – *Salpingoporella dinarica* RADOIČIĆ, 1959
- *Palorbitolina lenticularis* (BLUMENBACH, 1805)
- *Voloshinoides murgensis* LUPERTO SINNI & MASSE, 1993
- *Debarina hahounerensis* FOURCADE, RAOULT & VILA, 1972
- *Mesorbitolina parva* (DOUGLASS, 1960)
- 15 – *Mesorbitolina texana* (ROEMER, 1849)
- *Archaeoalveolina reicheli* (DE CASTRO, 1966)
- *Cuneolina parva* HENSON, 1948

The first and last occurrences (FO and LO) of these species are the basis of the most widely used biostratigraphic schemes for the central and southern Tethyan domain and their homotaxial order has been documented from the Apenninic, to the Adriatic-Dinaric to the Gavrovo-Tripolitza to the north African and Middle East carbonate Platforms

**Bio-  
chemostratigraphy of  
the Barremian-Aptian  
shallow-water**

M. Di Lucia et al.

Title Page

Abstract

Introduction

Conclusions

References

Tables

Figures

⏪

⏩

◀

▶

Back

Close

Full Screen / Esc

Printer-friendly Version

Interactive Discussion



(Chiocchini et al., 1994, 2008; Simmons, 1994; Husinec and Sokač, 2006; Velić, 2007; Tešović et al., 2011).

For the correlation of the studied successions we relied in particular on the following biostratigraphic markers that can be easily recognized also in the field:

1. The “*Archaeoalveolina reicheli* level”, represented by few meters of wackestone-packstones with abundant *A. reicheli*.
2. The “*Orbitolina* level”, a dm- to m-thick composite bed made by marls and marly limestones full of flat conical orbitolinids (*M. parva* and *M. texana*), topped by packstones with orbitolinids and codiacean green algae (*Boueina hochstetteri moncharmontiae* DE CASTRO, 1978) (Fig. 6).
3. The *Salpingoporella dinarica* acmes, represented by two distinct m-thick intervals of packstones crowded with *S. dinarica*, occurring a few meters below and above the “*Orbitolina* level” (Fig. 7).

### 4.3 Stratigraphy of the studied sections

#### 4.3.1 Mt. Croce

This succession was logged on the southern side of Mt. Croce in the Aurunci Mountains, about 17 km northwest of Formia (41°23'55" N, 13°31'45" E) (Fig. 2). It is 146.2m thick and has been divided into four intervals (A–D) on the basis of major changes in LA at the decametre scale (Fig. 8).

Interval A (0–45 m) shows a regular alternation of fenestral, mili-ostr-algal and biopeloidal limestones arranged in metric shallowing-upward (SU) cycles. In the first 20 m intertidal and supratidal facies prevail and subaerial exposure surfaces are well developed at the top of some SU cycles. The thickness of subtidal facies increases in the second half of this interval, marking the onset of a transgressive trend.

## Bio-chemostratigraphy of the Barremian-Aptian shallow-water

M. Di Lucia et al.

Title Page

Abstract

Introduction

Conclusions

References

Tables

Figures

⏪

⏩

◀

▶

Back

Close

Full Screen / Esc

Printer-friendly Version

Interactive Discussion

The lower part of Interval B (45–60 m) consists mainly of “Palorbitolina limestones”, with a few levels of requienid-gastropod floatstone and of foralgal wackestone-packstone. *Lithocodium/Bacinella* bindstones occur as dm-thick intercalations from 53.6 to 59.0 m. The upper part (60–75 m) is mainly made of for-algal wackestones/packstones alternating with a few levels of bio-peloidal packstone-grainstone. *Salpingoporella dinarica* wackestones-packstone are present at the top. Interval B terminates with a very prominent surface of subaerial exposure, marked by a lens of nodular marly limestones with rounded micritic clasts in a yellowish to greenish marly matrix.

Interval C (75–120 m) starts with the “Orbitolina level”, consisting of about 40 cm of marly limestones crowded with flat conical orbitolinids and codiaceans. The “Orbitolina level” is overlain by a few meters of fenestral mudstones and *S. dinarica* wackestones. From 79 to 84 m the quality of the outcrop is very poor. A few cm-thick beds of green marls are discontinuously exposed under a dense vegetation cover. The first beds after this covered interval consist of dm-thick levels of *S. dinarica* packstones. From about 87 to 112 m there are m-thick amalgamated beds of bio-peloidal packstone-grainstone, separated by thin levels of mili-ostr-algal mudstone-wackestone and for-algal wackestone. Interval C ends with dm-thick beds of bio-peloidal packstone-grainstone and for-algal wackestone-packstone, overlain by microbial/fenestral mudstones and chara-ostracodal mudstones-wackestones.

Interval D (120–146.2 m) consists of a regular alternation of dm-thick beds of mili-ostracodal mudstone-wackestone, for-algal wackestone and bio-peloidal packstone-grainstone. A few beds of partially dolomitized fenestral mudstone occur at the top of the interval.

The following biostratigraphic events have been recognized in the Mt. Croce section (Fig. 8):

- *P. infracretacea* occurs from the base to the top of the section.
- The FO of *S. dinarica* is at 4.6 m; the first acme is found at 69.8–79.8 m; the

## Bio- chemostratigraphy of the Barremian-Aptian shallow-water

M. Di Lucia et al.

Title Page

Abstract

Introduction

Conclusions

References

Tables

Figures

⏪

⏩

◀

▶

Back

Close

Full Screen / Esc

Printer-friendly Version

Interactive Discussion



second acme is at 86.8–87.8 m; the LO is at 95.4 m.

- The range of *P. lenticularis* spans from 45.0 to 60.2 m.
- The FO of *V. murgensis* is at 52.4 m; the LO at 65 m.
- *D. hahounerensis* occurs from 59 to 118 m.
- The “Orbitolina level” is found at 75.9–76.3 m. The first 20 cm contain exclusively *Mesorbitolina parva* and *M. texana*. The upper part contains also *B. hochstetteri moncharmontiae*.
- The FO of *A. reicheli* is at 112.3 m but the species becomes abundant from 117.9 to 118.8 m (*A. reicheli* level), in concomitance with the FO of *C. parva*.

### 4.3.2 Mt. Motola

This section was logged on the southern slope of Mt. Motola (40°21'53" N, 15°25'42" E), about 65 km southeast of Salerno (Fig. 9). It is 150.3 m thick and has been subdivided into four intervals. Interval A (0–75 m) consists mainly of biopeloidal packstones-grainstones, mili-ostr-algal mudstones-wackestones and microbial/fenestral mudstones. Two levels of for-algal packstone and requienid-gastropod floatstone occur in the uppermost part. The first 20 m are dominated by peritidal m-thick SU cycles. Subaerial exposure surfaces at the top of the cycles are marked by discontinuous levels of greenish/yellowish marls, infiltrating downwards into microkarstic cavities. Subtidal facies become predominant upwards, marking the onset of a deepening trend, but subaerial exposure surfaces are still present at the top of some cycles. Interval B (75–98 m) is dominated by subtidal facies. It consists mainly of *Palorbitolina* wackestones with sponge spicules and echinoderm fragments, alternating with requienid-gastropod floatstones. Cm- to dm-thick beds of *Lithocodium/Bacinella* bindstone are present at the base of this interval. A m-thick bed of packstone crowded

with nubecularid foraminifers occurs at the top. This interval terminates with a prominent subaerial exposure surface, marked by microkarstic cavities with greenish marly infilling.

At the base of interval C (98–126 m) there are about three meters of very poorly exposed section. Centimetric discontinuous marly levels are hardly visible under a thick vegetation and soil cover. The following beds are made of *S. dinarica* packstones alternating with 10 to 50 cm-thick levels of chara-ostracod and mili-ostr-algal mudstone-wackestone, capped by subaerial exposure surfaces. From 107 to 122 m, interval C consists mainly of very thick amalgamated beds (up to 6 m-thick) of bio-peloidal packstone-grainstone, with a few decimetric intercalations of gastropod-requienid floatstone. The uppermost part of the interval (122–126 m) is made of dm to m-thick beds of bio-peloidal packstone-grainstone alternating with microbial/fenestral mudstones capped by thin seams of marls, which infiltrates downward into microkarstic cavities. Interval D (126–150.3 m) is mainly made of bio-peloidal packstones-grainstones and mili-ostracodal mudstones-wackestones. Microbial/fenestral mudstones capped by subaerial exposure surfaces are present in the uppermost part of the section.

The following biostratigraphic events have been documented in the Mt. Motola section (Fig. 9):

- The FO of *P. infracretacea* is at 23 m; the range of this species extends beyond the top of this section.
- The FO of *S. dinarica* is at 27.6 m; the acme is at 103.5–104 m, the LO is at 109.6 m.
- The range of *P. lenticularis* spans from 79.2 to 89.7 m.
- The FO and LO of *V. murgensis* are placed at 84 and 89.7 m respectively.
- *D. hahounerensis* occurs from 85.4 to 137.3 m.
- The range of *A. reicheli* spans from 123 to 126.4 m; the maximum abundance (“*A. reicheli* level”) is observed at 125.1 to 126.4 m.

**Bio-  
chemostratigraphy of  
the Barremian-Aptian  
shallow-water**

M. Di Lucia et al.

Title Page

Abstract

Introduction

Conclusions

References

Tables

Figures



Back

Close

Full Screen / Esc

Printer-friendly Version

Interactive Discussion





mudstones. The uppermost five meters of interval C are almost entirely made of chara-ostracod mudstones and fenestral mudstones, capped by subaerial exposure surfaces. Interval D (119–135.2 m) is mainly made of an alternation of bio-peloidal packstones-grainstones and microbial/fenestral mudstones, with a few beds of mili-ostracod mudstone-wackestone. A couple of prominent subaerial exposure surfaces occur in the upper part of this interval.

The following biostratigraphic events were recognized in the Mt. Coccovello section (Fig. 10):

- *P. infracretacea* first occurs at 15.6 m and is present up to the top of the section.
- The FO of *S. dinarica* is at 42.3 m; its first acme is at 84.3 m, the second acme is at 94.5 m.
- *P. lenticularis* is present from 70.8 to 79.1 m.
- The FO and LO of *V. murgensis* are placed at 70.8 and 82.4 m respectively.
- *D. hahounerensis* occurs from 78.7 to 87 m.
- The base of the “Orbitolina level” is a 5 to 10 cm-thick discontinuous marly layer which occurs at 85.0 m above a prominent subaerial exposure surface and infiltrates downward into microkarstic cavities. This level contains *M. parva* and *M. texana*. Other cm-thick discontinuous marly levels with the same microfauna occur across a 5 m thick interval of poor exposure. The typical packstone with *Mesorbitolina* and the codiacean alga *B. hochstetteri moncharmontiae*, which elsewhere represents the top of the “Orbitolina level”, occurs at 91.2 m.
- The *A. reicheli* level corresponds to a 20 cm-thick layer at 110.8 m.

**Bio-  
chemostratigraphy of  
the Barremian-Aptian  
shallow-water**

M. Di Lucia et al.

Title Page

Abstract

Introduction

Conclusions

References

Tables

Figures



Back

Close

Full Screen / Esc

Printer-friendly Version

Interactive Discussion



## 4.4 Carbon and strontium isotope stratigraphy

### 4.4.1 Mt. Croce

One hundred and fifty samples were analyzed for the Mt. Croce section (Fig. 8). The lower part of the  $\delta^{13}\text{C}$  curve shows a rising trend with superimposed higher frequency fluctuations. Carbon isotope ratios increase from slightly negative values at the base of the section to a maximum of +2.1‰ at 39.1 m, about 6 m below the base of the “Palorbitolina limestones”. After a 1‰ decrease, the  $\delta^{13}\text{C}$  curve makes a plateau at about +1‰, which corresponds almost entirely to the “Palorbitolina limestones”. This plateau is followed by a marked positive excursion which starts 4 m below the top of the “Palorbitolina limestones”, peaks at about +3‰ and then decreases to pre-excursion values of +1‰ at 76.5 m, just above the “Orbitolina level”. From there it starts a new very broad positive excursion that peaks at about +4‰ 10 m above the second acme of *S. dinarica*, and returns at pre-excursion values 1 m above the *A. reicheli* level. The last part of the  $\delta^{13}\text{C}$  curve is characterized by values fluctuating between +1 and +2‰.

Three fragments of requienid shells from a floatstone at 57.4 m from the base of the section, 3 m below the top of the “Palorbitolina limestones”, have been analysed for strontium isotope stratigraphy (SIS). Their  $^{87}\text{Sr}/^{86}\text{Sr}$  mean value gives a numerical age of 124.1 Ma (Table 2).

### 4.4.2 Mt. Motola

One hundred and thirty-seven samples were analyzed for the Mt. Motola section (Fig. 9). The first part of the smoothed  $\delta^{13}\text{C}$  curve shows an overall rising trend, reaching a peak of about +2.2‰ at 62.6 m, about 16.6 m below the base of the “Palorbitolina limestones”. From this peak,  $\delta^{13}\text{C}$  values decrease and then make a plateau, roughly corresponding to the “Palorbitolina limestones”, defined by values fluctuating around +1‰. After a very sharp decrease to 0‰, there is a broad positive excursion, peaking at about +2.8‰ some 11 m above the acme of *S. dinarica* and returning at

SED

3, 789–838, 2011

## Bio- chemostratigraphy of the Barremian-Aptian shallow-water

M. Di Lucia et al.

Title Page

Abstract

Introduction

Conclusions

References

Tables

Figures

⏪

⏩

◀

▶

Back

Close

Full Screen / Esc

Printer-friendly Version

Interactive Discussion



values of about +1‰ 4 m above the *A. reicheli* level. The  $\delta^{13}\text{C}$  curve terminates with a rising trend to a peak of about +1.6‰.

#### 4.4.3 Mt. Coccovello

One hundred and twenty-nine samples were analyzed for the Mt. Coccovello section (Fig. 10). The first part of the  $\delta^{13}\text{C}$  smoothed curve shows an overall decreasing trend, from +0.3‰ at the base to -1.3‰ at 44 m, with superimposed higher frequency fluctuations. Then there is a rising trend, peaking at about +1.8‰ 8 m below the base of the “Palorbitolina limestones”. From this peak,  $\delta^{13}\text{C}$  values decrease to about +1‰ and stay around this value for most of the interval corresponding to the “Palorbitolina limestones”. Then there is a prominent positive excursion, peaking at +3.2‰ some 2 m above the top of the “Palorbitolina limestones” and declining to a minimum of +0.6‰ 0.5 m above the top of the “Orbitolina level”.

After a sharp positive shift to about +2.1‰, there is a very marked decrease to a minimum of -1.9‰, roughly corresponding to the *A. reicheli* level. The  $\delta^{13}\text{C}$  curve terminates with a rebound to -1‰, followed by a new decrease to -2.2‰.

Three fragments of requienid shells from a floatstone at 86.4 m from the base of the section, 1 m above the first level of marls with *Mesorbitolina*, have been analysed for SIS. Their  $^{87}\text{Sr}/^{86}\text{Sr}$  mean value gives a numerical age of 122.87 Ma (Table 2).

## 5 Discussion

### 5.1 Reliability of the $\delta^{13}\text{C}$ record

During the last two decades C-isotope stratigraphy has been successfully applied to high resolution dating and correlation of Cretaceous carbonate platform successions (Wagner, 1990; Jenkyns, 1995; Masse et al., 1999; Parente et al., 2007; Burla et al., 2008; Huck et al., 2011). On the other hand, it is well known that,

SED

3, 789–838, 2011

## Bio- chemostratigraphy of the Barremian-Aptian shallow-water

M. Di Lucia et al.

Title Page

Abstract

Introduction

Conclusions

References

Tables

Figures

⏪

⏩

◀

▶

Back

Close

Full Screen / Esc

Printer-friendly Version

Interactive Discussion



## Bio-chemostratigraphy of the Barremian-Aptian shallow-water

M. Di Lucia et al.

Title Page

Abstract

Introduction

Conclusions

References

Tables

Figures

⏪

⏩

◀

▶

Back

Close

Full Screen / Esc

Printer-friendly Version

Interactive Discussion

besides post-depositional diagenetic alteration (Dickson and Coleman, 1980; Allan and Matthews, 1982; Lohmann, 1988; Marshall, 1992), biological fractionation and local palaeoceanographic conditions may cause the carbon isotope signal of platform carbonates to deviate from the open ocean global signal (Weber and Woodhead, 1969; Patterson and Walter, 1994; see Immenhauser et al., 2008, for a recent review). A recent study concluded that, in Kimmeridgian shallow water carbonates of the Jura Mountains, the general trend of  $\delta^{13}\text{C}$  values faithfully record the long-term global variations of the open ocean while higher order fluctuations “might result from variations in local environmental conditions on the shallow platform” (Colombié et al., 2011).

Therefore, before attempting a correlation with the reference curves of pelagic and hemipelagic successions, we tried to assess if the stable isotope record of the studied successions is significantly biased by diagenesis and/or by local environmental conditions.

Sub-aerial exposure surfaces are typically characterized by extreme depletions in the  $\delta^{13}\text{C}$ , while diagenesis in the vadose zone is generally characterized by depleted  $\delta^{18}\text{O}$  values and highly variable  $\delta^{13}\text{C}$ . Strong covariation between  $\delta^{13}\text{C}$  and  $\delta^{18}\text{O}$  is generally taken as proof of diagenetic alteration of the stable isotope signal under the influx of meteoric water in the mixing zone (Allan and Matthews, 1982). The scatter plots of carbon and oxygen isotope ratios (Fig. 11) show that the covariance between  $\delta^{13}\text{C}$  and  $\delta^{18}\text{O}$  values is very low to moderate for the three studied sections ( $r = 0.18 - 0.30$ ). However, some lithofacies associations show higher correlation coefficients (Table 3) that could be partly the result of mixing-zone diagenesis. Some very negative  $\delta^{13}\text{C}$  values, especially at Monte Coccovello, are associated with subaerial exposure surfaces and depleted  $\delta^{18}\text{O}$  values, especially at Monte Motola, are seemingly due to vadose diagenesis. Summing up, the effects of diagenesis are certainly seen in our isotopic records. They are probably responsible for some high-frequency fluctuations, defined by one or a few data points, but they are not so pervasive as to distort completely the pristine marine signal.

## Bio-chemostratigraphy of the Barremian-Aptian shallow-water

M. Di Lucia et al.

Title Page

Abstract

Introduction

Conclusions

References

Tables

Figures

⏪

⏩

◀

▶

Back

Close

Full Screen / Esc

Printer-friendly Version

Interactive Discussion

On the other hand, the scatter plots show also that there is no clear separation between the data points of the different lithofacies associations. This suggests that variations in  $\delta^{13}\text{C}$  cannot be related solely to facies changes. The bias of local palaeoenvironmental conditions could have been partly counteracted by the fact that we did not use bulk samples but strived to sample the micritic matrix also in the grainy facies. On the other hand, the lack of a strict relationship between facies type and  $\delta^{13}\text{C}$  has been observed also in the recent sediments of the Great Bahama Bank (Swart et al., 2009).

The  $\delta^{13}\text{C}$  and  $\delta^{18}\text{O}$  mean values for the three studied successions fall within the range of Barremian–Aptian seawater (taken from the “low-latitude” biotic calcite record of Prokoph et al., 2008). A significant tail of more negative values is only observed for the Mt. Coccovello section. The same pattern of more negative values in the most restricted section has been observed also in the Cenomanian–Turonian platform carbonates of the Apenninic platform (Parente et al., 2007).

The smoothed  $\delta^{13}\text{C}$  curves of Figs. 8 to 10 show that, besides the higher order fluctuations at metric to sub-metric scale, defined by only one or a few points, there are some isotopic trends and excursions which are defined by many data points and extend across intervals that are tens of meters thick. These major features of the  $\delta^{13}\text{C}$  curves are statistically significant because, at least in the Mt. Croce and Mt. Motola sections, they represent deviations from the mean value that are 2–3 times the standard deviation. Moreover, they persist across changes of lithofacies association, suggesting that they are not caused by local changes of palaeoenvironmental conditions. Finally, as discussed in the next paragraph, the major trends and excursions can be correlated between the three studied sections, suggesting that the forcing was, if not global, at least regional.

### 5.2 Platform-to-basin chemostratigraphic correlation

Under the hypothesis that the carbon isotope record of the three studied sections was not entirely shaped by local palaeoenvironmental changes and diagenetic overprint, we attempted a chemostratigraphic correlation with the reference carbon isotope curve

of the Cismon Apticore in the southern Alps (Menegatti et al., 1998; Erba et al., 1999) and with the composite curve compiled by Föllmi et al. (2006) for the Vocontian Basin of south-eastern France. For the nomenclature of the isotopic segments we refer to Wissler et al. (2003) for the Barremian–Early Aptian interval (B3–B8/A1–A3) and to Menegatti et al. (1998) for the isotopic excursion of the Selli event (C3–C7) (Fig. 12).

The most significant feature of the carbon isotope curves of the studied sections is the very prominent positive excursion (about 2.5–3‰) which starts 0.4 m above the “Orbitolina level” at Mt. Croce and terminates 1 m above the “*A. reicheli* level”. By correlating the “*A. reicheli* level” and the acme of *S. dinarica*, the same excursion can be recognized in the Mt. Motola  $\delta^{13}\text{C}$  curve, between 96.4 and 137.3 m. In the Mt. Coccovello section this positive excursion is poorly developed, because of poor resolution of this segment of the curve and because of a gap, truncating the uppermost part of the *S. dinarica* range.

We correlate this positive excursion with the isotopic excursion corresponding to segments C4–C7 in the Cismon Apticore curve. According to the calibration of Föllmi et al. (2006), this positive excursion spans from the Lower Aptian *D. deshayesi* zone (very close to the boundary with the *D. weissii* zone) to the uppermost part of the Upper Aptian *E. subnodosocostatum* ammonite zone.

Our chemostratigraphic correlation is supported by the following independent tie-points:

1. An Upper Aptian (Gargasian) age for *A. reicheli*, constrained by ammonites in the carbonate platforms of North Africa (Fourcade and Raoult, 1973; Bismuth, 1973; Cherchi and Schroeder, 1982; but see Chihaoui et al., 2010, for a partly different view).
2. A numerical age of 122.9 Ma (122.1–123.5), obtained by SIS for a requienid floatstone 1 m above the first marls with *Mesorbitolina* at Mt. Coccovello. This age should correspond to the *D. weissii* ammonite zone, even if the calibration between SIS numerical ages and the ammonite zonation has been recently questioned for

**Bio-  
chemostratigraphy of  
the Barremian-Aptian  
shallow-water**

M. Di Lucia et al.

Title Page

Abstract

Introduction

Conclusions

References

Tables

Figures

◀

▶

◀

▶

Back

Close

Full Screen / Esc

Printer-friendly Version

Interactive Discussion



the Lower Aptian interval (Huck et al., 2011).

Building upon this correlation, the negative spike limiting the onset of the positive excursion is equated to the C3 negative spike of Menegatti et al. (1998). The decreasing trend observed both at Monte Croce and at Monte Coccovello is reminiscent of the gradual decrease observed at Cassis la Bedoule (Kuhnt et al., 2011) and at Pusiano (Keller et al., 2011), lending further support to the hypothesis that the very sharp decrease observed in the Cismon core might be partly due to condensation or to a small gap.

The positive excursion of the Selli event is preceded at Mt. Croce by another positive excursion (about 2‰ in amplitude) which culminates at 64.2 m, 4 m above the LO of *P. lenticularis*. The same excursion is recognized at Mt. Coccovello between 75.2 and 92.1 m. At Mt. Motola the isotopic record is distorted by a stratigraphic gap, supported by sedimentologic evidence of prolonged subaerial exposure at 98.0 m (Fig. 9) and confirmed by the absence of the first *S. dinarica* acme and of the “Orbitolina level”. The rising limb of this positive excursion is correlated with the A1–A2 segments of Wissler et al. (2003), spanning from the Barremian–Aptian boundary to the lowermost Aptian. This correlation is supported by the SIS numerical age of  $124.1 \pm 1.1$  Ma, corresponding to the *D. oglanlensis* ammonite zone, of a requienid level occurring 3 m below the LO of *P. lenticularis* at Mt. Croce. Accordingly, the distinctive negative trend, seen in all the three sections below this positive excursion, has been equated to the B7–B8 segments of Wissler et al. (2003).

Chemostratigraphic correlation becomes less compelling for the lower part of the studied sections, mainly because of the lack of independent tie-points and because of the small amplitude of isotopic excursions in the reference curves (<1‰). Nevertheless, a tentative correlation is supplied in Fig. 12, which suggests that the lowermost part of the Mt. Motola and Mt. Coccovello sections might extend into the Lower Barremian.

**Bio-  
chemostratigraphy of  
the Barremian-Aptian  
shallow-water**

M. Di Lucia et al.

Title Page

Abstract

Introduction

Conclusions

References

Tables

Figures



Back

Close

Full Screen / Esc

Printer-friendly Version

Interactive Discussion



### 5.3 Biostratigraphic criteria for the Selli event in central Tethyan carbonate platforms

Chemostratigraphic correlation with the well dated carbon isotope curves of the Cismon core and of the Vocontian composite section allows individuating in the carbonate platform successions of the southern Apennines the segments corresponding to the OAE1a. This opens the possibility of investigating the response of the resilient Apenninic carbonate platform to the palaeoenvironmental perturbations associated with events like the nannoconid biocalcification crisis (corresponding to the C3 segment of the carbon isotope curve, Erba et al., 2010) and the Selli event of enhanced organic carbon burial (corresponding to the C4–C6 interval). This is the object of a companion paper. In this paper we propose a set of biostratigraphic criteria to individuate the stratigraphic interval equivalent to the OAE1a in the carbonate platforms of the central and southern Tethys. These criteria will be particularly useful when carbon isotope stratigraphy is not available or when chemostratigraphic correlation is biased by low resolution or by the overprint of local palaeoceanographic processes and/or of early meteoric diagenesis. A survey of the recent literature shows that this is often the case in shallow-water carbonate sections. For instance, some recently published carbon isotope curves from the Barremian–Aptian of the Adriatic-Dinaric carbonate platform show no evidence of the broad positive excursion associated with the Selli event and of the preceding negative shift (Tešović et al., 2011). In another case study, the OAE1a positive CIE is not present in the carbon isotope record of bulk/micritic matrix samples, while it is faithfully reproduced by the biotic calcite of rudist shells (Huck et al., 2010). Poorly defined CIEs have been recovered also from some Barremian–Aptian sections of the southern Apenninic carbonate platform (D’Argenio et al., 2004).

Based on the chemostratigraphic correlation of Fig. 12, the Selli level (C4–C6 segments of the carbon isotope curve) corresponds in the southern Apenninic carbonate platform to the interval between the “Orbitolina level” and the second acme of *S. dinarica*. The biocalcification crisis (C3 segment of the carbon isotope curve), highlighted

SED

3, 789–838, 2011

#### Bio-chemostratigraphy of the Barremian-Aptian shallow-water

M. Di Lucia et al.

Title Page

Abstract

Introduction

Conclusions

References

Tables

Figures

⏪

⏩

◀

▶

Back

Close

Full Screen / Esc

Printer-friendly Version

Interactive Discussion



by nannoconids in the deep-water record, corresponds to the interval going from the first acme of *S. dinarica* to just above the top of the “Orbitolina level”.

These biostratigraphic events are particularly suitable because they are widely used in the most popular biostratigraphic schemes of central and southern Tethyan carbonate platforms (Simmons, 1994; Velić, 2007; Chiocchini et al., 2008). In particular, the “Orbitolina level” is used as a lithostratigraphic marker in the geological maps of central and southern Apennines. Also the acme of *S. dinarica* is easily picked in the field and is widely recognized in central Tethyan carbonate platforms.

#### 5.4 Chronostratigraphic calibration of carbonate platform biostratigraphy

The biozonations of the Lower Cretaceous carbonate platforms of the central Tethys (Apenninic, Adriatic and Gavrovo-Tripolitza platforms) are mainly based on calcareous algae and larger benthic foraminifera. The chronostratigraphic calibration of these schemes has always posed serious problems because ammonites, and calcareous plankton and nannoplankton, which are the pillars of Cretaceous chronostratigraphy, are notably absent from carbonate platform successions.

The problem of chronostratigraphic calibration has been explicitly acknowledged by some authors (De Castro, 1991; Chiocchini et al., 2008). Others (Bachmann and Hirsch, 2006; Velić, 2007) have anchored their biostratigraphic schemes to the chronostratigraphic ages of orbitolinid larger foraminifera, which have been established mainly in Northern Tethyan carbonate platforms.

We highlight several shortcomings in this indirect correlation:

- The precise isochrony of FOs and LOs of orbitolinid species between the northern and central-southern carbonate platforms has been never tested against independent evidence.
- Orbitolinids are generally found in discrete intervals and sometimes are totally lacking in inner platform facies. Namely, the flat conical species are generally

Title Page

Abstract

Introduction

Conclusions

References

Tables

Figures



Back

Close

Full Screen / Esc

Printer-friendly Version

Interactive Discussion



**Bio-chemostratigraphy of the Barremian-Aptian shallow-water**

M. Di Lucia et al.

Title Page

Abstract

Introduction

Conclusions

References

Tables

Figures



Back

Close

Full Screen / Esc

Printer-friendly Version

Interactive Discussion



found in marly or calcareous marly levels, which seemingly represent transgressive to maximum flooding intervals. The local range of these taxa could be related more to the occurrence of the appropriate facies, controlled by local to regional sea-level history, than to evolutionary processes of speciation and extinction.

- 5 – The chronostratigraphic calibration of orbitolinid biostratigraphy is still the matter of intense scientific debate, even in the areas where it has been first proposed, like the Urgonian platforms of the northern Tethyan margin (Arnaud et al., 1998; Clavel et al., 2007; Föllmi, 2008; Conrad et al., 2011; Godét et al., 2011).

For all these reasons, we advocate the supremacy of chemostratigraphic correlation, used in this paper, to establishing the chronostratigraphic calibration of carbonate platform biostratigraphy.

The high-resolution chemostratigraphic correlation with the well-dated reference sections of the Cismon Apticore and of the Vocontian basin of south-eastern France is here used to establishing the chronostratigraphic age of the biostratigraphic events recognized in the carbonate platform successions of the southern Apennines (Fig. 12). We refer to the lowest FO and to the highest LO, assuming that the small differences between the ranges observed in the three studied sections are the result of the lack of appropriate facies, of small gaps or of other sampling biases.

- 20 – The FO of *P. infracretacea* correlates with the base of the Upper Barremian (*H. uhligi* ammonite zone). This species persists until the top of the three studied sections.
- The range of *P. lenticularis* spans from the uppermost Barremian (*C. sarasini* zone) to the lowermost Aptian (upper part of the *D. oglanlensis* zone). In all the three studied sections levels rich of *P. lenticularis* (LA8, “Palorbitolina limestones”) mark a transgressive interval corresponding to the B8–A1 segments of the carbon isotope curves. Therefore, chemostratigraphy supports a correlation of the “Palorbitolina limestones” of southern Apennines with the “Couches inférieures

## Bio- chemostratigraphy of the Barremian-Aptian shallow-water

M. Di Lucia et al.

Title Page

Abstract

Introduction

Conclusions

References

Tables

Figures

◀

▶

◀

▶

Back

Close

Full Screen / Esc

Printer-friendly Version

Interactive Discussion



à Orbitolines” of the French Vercors and with the “Lower Orbitolina Beds” of the northern Tethyan Helvetic platform (Arnaud et al., 1998; Clavel et al., 2002; Föllmi et al., 2007; Föllmi and Gainon, 2008).

- The range of *V. murgensis* encompasses the Barremian–Aptian boundary (FO in the upper part of the *C. sarasini* zone, LO in the lower part of the *D. weissii* zone).
- The FO of *D. hahounerensis* correlates with the base of the Aptian (*D. oglanlensis* ammonite zone). The LO of *D. hahounerensis* correlates with the Upper Aptian *E. subnodosocostatum* ammonite zone.
- The first acme of *S. dinarica* falls within the *D. weissii* zone, while the second acme is correlated with the upper part of the *D. deshayesi* zone. Therefore, the interval of maximum abundance of this dasyclad alga in the southern Apennines is in the Lower Aptian. Rare specimens are observed in levels correlated with the Upper Barremian, while the highest LO is observed in levels correlated with the *D. furcata* ammonite zone. In the Adriatic carbonate platform(s) the interval of maximum abundance of *S. dinarica* is placed in the Upper Aptian, but this chronostratigraphic age is anchored to the age attributed to the FO of *M. parva* and *M. texana* (see the discussion below).
- The “Orbitolina level” of the southern Apennines correlates with the boundary interval between the *D. weissii* and the *D. deshayesi* zones, in the Lower Aptian. This level, containing an association of *M. parva* and *M. texana* (Fig. 5), has been so far attributed to the Gargasian (Cherchi et al., 1978). The Gargasian age of the FO of *M. texana*, recently restated by Schroeder et al. (2010), is one of the tie points for the calibration of the Aptian biostratigraphy of central and southern Tethyan carbonate platforms (Simmons, 1994; Witt and Gökdağ, 1994; Bachmann and Hirsch, 2006; Velić, 2007). However, in the northern tethyan Helvetic carbonate platform *M. texana* has been found in the upper Schratteknalk Fm. (Schroeder in Schenk, 2002; Schroeder et al., 2007), which has been dated

## Bio- chemostratigraphy of the Barremian-Aptian shallow-water

M. Di Lucia et al.

Title Page

Abstract

Introduction

Conclusions

References

Tables

Figures

⏪

⏩

◀

▶

Back

Close

Full Screen / Esc

Printer-friendly Version

Interactive Discussion



by carbon isotope stratigraphy and ammonites as middle Early Aptian, close to the boundary between the *D. weissii* and the *D. deshayesi* zones (Föllmi, 2008; Föllmi and Gainon, 2008). These data agree with our chemostratigraphically constrained chronostratigraphic calibration and suggest a correlation between the “Orbitolina level” of the southern Apennines, the “Couches supérieures à orbitolines” of the French Vercors and the “Upper Orbitolina Beds” of the Helvetic Alps (Linder et al., 2006; Föllmi and Gainon, 2008).

- The *A. reicheli* level is correlated with the upper part of the *E. subnodosocostatum* zone (Gargasian, Upper Aptian). This calibration is in accordance with the age supported by ammonites in some sections of the Northern African carbonate platforms (Bismuth, 1973; Fourcade and Raoult, 1973; Cherchi and Schroeder, 1982) but we acknowledge that the chronostratigraphic age of these sections is still under debate (Cherchi and Schroeder, 1982; Chihaoui et al., 2010).
- The FO of *C. parva* is correlated with the upper part of the *E. subnodosocostatum* zone, in the Upper Aptian.

In the scheme of Fig. 13, the chronostratigraphic ranges supported by our chemostratigraphic correlation are compared with the ranges given for the same species in other biostratigraphic schemes of central and southern Tethyan carbonate platforms (Bachmann and Hirsch, 2006; Husinec and Sokač, 2006; Velić, 2007; Chiocchini et al., 2008; Tešović et al., 2011). Several discrepancies emerge, some of which have been already discussed above. Some of these discrepancies might be due to a slight diachroneity of the biostratigraphic events between different carbonate platforms. However, it must be re-emphasized that for all the biostratigraphic schemes (but ours) the chronostratigraphic calibration is largely based on the ages proposed for orbitolinids in the carbonate platforms of the Northern Tethyan margin. This indirect chronostratigraphic calibration might be biased for several reasons, as discussed above.

## 6 Conclusions

The geological archive of the resilient central and southern Tethyan carbonate platforms contains valuable information on the response of tropical and subtropical neritic ecosystems to the palaeoenvironmental perturbations associated with the massive injection of CO<sub>2</sub> into the Atmosphere–Ocean system during the early Aptian OAE1a. The first step to unlock this archive is the precise chronostratigraphic dating and correlation of shallow-water carbonate successions with deep-water successions, which represent the reference record of palaeoceanographic events. In this paper we fulfil this task by integrating high-resolution carbon isotope stratigraphy and biostratigraphy, with additional support by strontium isotope stratigraphy on a limited set of samples. Chemostratigraphic correlation of three successions of the Apenninic carbonate platform of southern Italy with the Cismon Apticore and the composite section of the Vocontian Basin permits the chronostratigraphic calibration of carbonate platform biostratigraphy across the Barremian–Aptian interval.

The main result derived from this calibration is the definition of biostratigraphic criteria to individuate, in the carbonate platforms of the central and southern Tethys, the stratigraphic interval equivalent to the main palaeoceanographic events associated with the OAE1a. The interval of enhanced organic carbon accumulation in deep-water reference successions (C4–C6 segments of the carbon isotope curve) corresponds in the southern Apenninic carbonate platform to the interval between the “Orbitolina level” and the second acme of *S. dinarica*. The biocalcification crisis of nannoconids (C3 segment of the carbon isotope curve), corresponds to the interval going from the first acme of *S. dinarica* to just above the top of the “Orbitolina level”.

These criteria are particularly valuable because they are based on biostratigraphic events that are routinely utilized in central and southern Tethyan carbonate platforms. They offer a useful alternative when carbon isotope stratigraphy is not available or fails to produce a reliable correlation with the reference curves, which is unfortunately very common in carbonate platform successions.

### Bio-chemostratigraphy of the Barremian-Aptian shallow-water

M. Di Lucia et al.

Title Page

Abstract

Introduction

Conclusions

References

Tables

Figures



Back

Close

Full Screen / Esc

Printer-friendly Version

Interactive Discussion





## References

- Allan, J. R. and Matthews, R. K.: Isotope signature associated with early meteoric diagenesis, *Sedimentology*, 29, 797–897, 1982.
- Arnaud, H., Arnaud-Vanneau, A., Blanc-Alétru, M.-C., Adatte, T., Argot, M., Delanoy, G., Thieuloy, J.-P., Vermeulen, J., Virgone, A., Virlouvét, B., and Wermeille, S.: Répartition stratigraphique des orbitolinidés de la plate-forme urgonienne subalpine et jurassienne (SE de la France), *Géologie Alpine*, 74, 3–89, 1998.
- Arthur, M. A., Brumsack, H.-J., Jenkyns, H. C., and Schlanger, S. O.: Stratigraphy, geochemistry, and paleoceanography of organic carbon-rich Cretaceous sequences, edited by: Ginsburg, N. and Baudoin, B., *Cretaceous Resources, Events and Rhythms*, Kluwer, Dordrecht, 75–119, 1990.
- Bachmann, M. and Hirsch, F.: Lower Cretaceous carbonate platform of the eastern Levant (Galilee and the Golan Heights): stratigraphy and second-order sea-level change. *Cret. Res.*, 27, 487–512, 2006.
- Bismuth, H.: Réflexions stratigraphiques sur l'Albo-Aptien dans la région des djebels Douleb et Semmama et son environnement (Tunisie du Centre-Nord), *Annales des Mines et de la Géologie, Livre Jubilaire M. Solignac, Tunis*, 6, 179–212, 1973.
- Bonardi, G., D'Argenio, B., and Perrone, V.: *Carta Geologica dell'Appennino meridionale, SELCA*, Firenze, 1988.
- Bosellini, A.: Dinosaurs “re-write” the geodynamics of the eastern Mediterranean and the paleogeography of the Apulia Platform, *Earth Sci. Rev.*, 59, 211–234, 2002.
- Burla, S., Heimhofer, U., Hochuli, P. A., Weissert, H., and Skelton, P.: Changes in sedimentary patterns of coastal and deep sea successions from the North Atlantic (Portugal) linked to Early Cretaceous environmental change, *Palaeogeogr. Palaeocl.*, 257, 38–57, 2008.
- Carannante, G., Graziano, R., Ruberti, D., and Simone, L.: Upper Cretaceous temperate-type open shelves from northern (Sardinia) and southern (Apennines-Apulia) Mesozoic Tethyan margins, in: *Cool-water carbonates*, edited by: James, N. P. and Clarke, J., *SEPM Spec. P.*, 56, 309–325, 1997.
- Cherchi, A. and Schroeder, R.: *Dictyoconus algerianus* n. sp., grand foraminifère de l'Aptien supérieur de la plaque africaine (marge septentrionale), *Comptes rendus de l'Académie des Sciences de Paris*, II, 295, 77–82, 1982.
- Cherchi, A., De Castro, P., and Schroeder, R.: Sull'età dei livelli a Orbitolinidi della Campania e

SED

3, 789–838, 2011

### Bio- chemostratigraphy of the Barremian-Aptian shallow-water

M. Di Lucia et al.

Title Page

Abstract

Introduction

Conclusions

References

Tables

Figures

◀

▶

◀

▶

Back

Close

Full Screen / Esc

Printer-friendly Version

Interactive Discussion





## Bio- chemostratigraphy of the Barremian-Aptian shallow-water

M. Di Lucia et al.

[Title Page](#)[Abstract](#)[Introduction](#)[Conclusions](#)[References](#)[Tables](#)[Figures](#)[⏪](#)[⏩](#)[◀](#)[▶](#)[Back](#)[Close](#)[Full Screen / Esc](#)[Printer-friendly Version](#)[Interactive Discussion](#)

of identical lithofacies and age, AAPG Bull., 59, 524–533, 1975.

D'Argenio, B., Ferreri, V., Weissert, H., Amodio, S., Buonocunto, F. P., and Wissler, L.: A multidisciplinary approach to global correlation and geochronology: the Cretaceous shallow-water carbonates of southern Apennines, Italy, in: Cyclostratigraphy: Approaches and Case Histories, edited by: D'Argenio, B., Fischer, A.G., Premoli Silva I., Weissert, H. and Ferreri, V., SEPM Spec. P., 81, 103–122, 2004.

De Castro, P.: Contributo alla conoscenza delle Alveoline albiano–cenomaniane della Campania, Boll. Soc. Nat., Napoli, 75, 219–275, 1966.

De Castro, P.: Mesozoic, in: 5th International Symposium on Fossil Algae, edited by: Barattolo, F., De Castro, P., and Parente, M., Field Trip Guide-Book, Giannini, Napoli, 21–38, 1991.

Dickson, J. A. D. and Coleman, M. L.: Changes in carbon and oxygen isotope composition during limestone diagenesis, Sedimentology, 27, 107–118, 1980.

Erba, E., Channell, J. E. T., Claps, M., Jones, C., Larson, R. L., Opdyke, B. N., Silva, I. P., Riva, A., Salvini, G., and Torricelli, S.: Integrated stratigraphy of the Cismon APTICORE (Southern Alps, Italy): a “reference section” for the Barremian–Aptian interval at low latitudes, J. Foramin. Res., 29, 371–391, 1999.

Erba, E., Bottini, C., Weissert, H. J., and Keller, C. E.: Calcareous Nannoplankton Response to Surface-Water Acidification around Oceanic Anoxic Event 1a, Science, 329, 428–432, 2010.

Föllmi, K. B.: A synchronous, middle Early Aptian age for the demise of the Helvetic Urganian platform related to the unfolding oceanic anoxic event 1a (“Selli event”), Revue de Paléobiologie, Genève, 27, 2, 461–468, 2008.

Föllmi, K. B. and Gainon, F.: Demise of the northern Tethyan Urganian carbonate platform and subsequent transition towards pelagic conditions: the sedimentary record of the Col de la Plaine Morte area, central Switzerland, Sediment. Geol., 205, 142–159, 2008.

Föllmi, K. B., Godet, A., Bodin, S., and Linder, P.: Interactions between environmental change and shallow water carbonate buildup along the northern Tethyan margin and their impact on the Early Cretaceous carbon isotope record, Paleocyanography, 21, 4211–4216, 2006.

Föllmi, K. B., Bodin, S., Godet, A., Linder, P., and van de Schootbrugge, B.: Unlocking paleo-environmental information from early Cretaceous shelf sediments in the Helvetic Alps: stratigraphy is the key!, Swiss J. Geosci., 100, 349–369, 2007.

Fourcade, E. and Raoult, J.-F.: Crétacé du Kef Hahouner et position stratigraphique de “Ovalveolina” reicheli P. de Castro (série septentrionale du môle néritique du Constantinois, Algérie), Revue de Micropaléontologie, 15, 4, 227–246, 1973.



## Bio-chemostratigraphy of the Barremian-Aptian shallow-water

M. Di Lucia et al.

Title Page

Abstract

Introduction

Conclusions

References

Tables

Figures

◀

▶

◀

▶

Back

Close

Full Screen / Esc

Printer-friendly Version

Interactive Discussion



oceanic anoxic event 1a, *Sedimentology*, 52, 77–99, 2005.

Immenhauser, A., Holmden, C., and Patterson, W. P.: Interpreting the Carbon-Isotope Record of Ancient Shallow Epeiric Seas: Lessons from the Recent, in: *Dynamics of Epeiric Seas*, edited by: Pratt, B. R. and Holmden, C., Geological Association of Canada Special Publication, 48, 135–174, 2008.

Jenkyns, H. C.: Carbon-isotope stratigraphy and paleoceanographic significance of the Lower Cretaceous shallow-water carbonates of Resolution Guyot, mid-Pacific Mountains, in: *Proceedings of the Ocean Drilling Program, Scientific Results*, 143, edited by: Winterer, E. L., Sager, W. W., Firth, J. V. and Sinton, J. M., Ocean Drilling Program, College Station, TX, 99–104, 1995.

Keller, C. E., Hochuli, P. A., Weissert, H., Bernasconi, S. M., Giorgioni, M., Garcia, T. I.: A volcanically induced climate warming and floral change preceded the onset of OAE1a (Early Cretaceous), *Palaeogeogr., Palaeoclimatol.*, 305, 43–49, doi:10.1016/j.palaeo.2011.02.011, 2011.

Kuhnt, W., Holbourn, A., and Moullade, M.: Transient global cooling at the onset of early Aptian oceanic anoxic event (OAE) 1a, *Geology*, 39, 323–326, doi:10.1130/G31554.1, 2011.

Larson, R. L. and Erba, E.: Onset of the mid-Cretaceous greenhouse in the Barremian–Aptian: Igneous events and the biological, sedimentary, and geochemical responses, *Paleoceanography*, 14, 663–678, 1999.

Linder, P., Gigandet, J., Hüsser, J. L., Gainon, F., and Föllmi, K. B.: The early Aptian Grönten Member: description of a new lithostratigraphic unit of the Helvetic Garschella Formation, *Eclogae Geol. Helv.*, 99, 327–341, 2006.

Lohmann, K. C.: Geochemical patterns of meteoric diagenetic systems and their application to studies of paleokarst, in: *Paleokarst.*, edited by: James, N. P. and Choquette, P. W., Springer, Berlin, 58–80, 1988.

Marshall, J. D.: Climatic and oceanographic isotopic signals from the carbonate rock record and their preservation, *Geol. Mag.*, 129, 143–160, 1992.

Masse, J. P., El Albani, A., and Erlenkeuser, H.: Stratigraphie isotopique ( $\delta^{13}\text{C}$ ) de l'Aptien inférieur de Provence (SE France): Application aux corrélations plate-forme/bassin, *Eclogae Geol. Helv.*, 92, 259–263, 1999.

McArthur, J. M., Howarth, R. J., and Bailey, T. R.: Strontium Isotope Stratigraphy: LOWESS Version 3: best fit to the marine Sr-Isotope Curve for 0–509 Ma and accompanying look-up table for deriving numerical age, *J. Geol.*, 109, 155–170, 2001.

Méhay, S., Keller, C. E., Bernasconi, S. M., Weissert, H., Erba, E., Bottini, C., and Hochuli, P.

## Bio- chemostratigraphy of the Barremian-Aptian shallow-water

M. Di Lucia et al.

[Title Page](#)
[Abstract](#)
[Introduction](#)
[Conclusions](#)
[References](#)
[Tables](#)
[Figures](#)




[Back](#)
[Close](#)
[Full Screen / Esc](#)
[Printer-friendly Version](#)
[Interactive Discussion](#)


A.: A volcanic CO<sub>2</sub> pulse triggered the Cretaceous Oceanic Anoxic Event 1a and a biocalcification crisis, *Geology*, 37, 819–822, 2009.

Menegatti, A. P., Weissert, H., Brown, R. S., Tyson, R. V., Farrimond, P., Strasser, A., and Caron, M.: High-resolution δ<sup>13</sup>C stratigraphy through the early Aptian “Livello Selli” of the Alpine Tethys, *Paleoceanography*, 13, 530–545, 1998.

Parente, M., Frijia, G., and Di Lucia, M.: Carbon-isotope stratigraphy of Cenomanian–Turonian platform carbonates from southern Apennines (Italy): a chemostratigraphic approach to the problem of correlation between shallow-water and deep-water successions, *J. Geol. Soc. Lond.*, 164, 609–620, 2007.

Patterson, W. P. and Walter, L. M.: Depletion of <sup>13</sup>C in seawater δCO<sub>2</sub> on modern carbonate platforms: significance for the carbon isotopic record of carbonates, *Geology*, 22, 885–888, 1994.

Pittet, B., van Buchem, F. S. P., Hillgärtner, H., Razin, P., Grötsch, J., and Droste, H. J.: Ecological succession, palaeoenvironmental change, and depositional sequences of Barremian–Aptian shallow-water carbonates in northern Oman, *Sedimentology*, 49, 555–581, 2002.

Prokoph, A., Shields, G. A., and Veizer, J.: Compilation and time-series analysis of a marine carbonate δ<sup>18</sup>O, δ<sup>13</sup>C, <sup>87</sup>Sr/<sup>86</sup>Sr and δ<sup>34</sup>S database through Earth history, *Earth Sci. Rev.*, 87, 113–133, 2008.

Raspini, A.: Stacking pattern of cyclic carbonate platform strata: Lower Cretaceous of southern Apennines, Italy, *J. Geol. Soc. Lond.*, 158, 353–366, 2001.

Sartoni, S. and Crescenti, U.: Ricerche biostratigrafiche nel Mesozoico dell’Appennino meridionale, *Giornale di Geologia*, 29, 161–293, 1962.

Schenk, K.: Die Drusberg- und Schratzenkalk-Formation (Unterkreide) im Helvetikum des Berner Oberlandes, Unpublished PhD Thesis, University of Berne, 1992.

Schroeder, R., Schenk, K., Cherchi, A., and Schwizer, B.: Sur la présence de grands foraminifères d’âge aptien supérieur dans l’Urgonien de la Nappe du Wildhorn (Suisse centrale), Note préliminaire, *Revue de Paléobiologie*, 26, 665–669, 2007.

Schroeder, R., van Buchem, F. S. P., Cherchi, A., Baghbani, D., Vincent, B., Immenhauser, A., and Granier, B.: Revised orbitolinid biostratigraphic zonation for the Barremian–Aptian of the eastern Arabian Plate and implications for regional stratigraphic correlations, *GeoArabia Special Publication*, 4, 1, 49–96, 2010.

Simmons, M. D.: Micropalaeontological biozonation of the Kahmah Group (Early Cretaceous), Central Oman Mountains, in: *Micropalaeontology and Hydrocarbon Exploration in the Middle*

## Bio-chemostratigraphy of the Barremian-Aptian shallow-water

M. Di Lucia et al.

Title Page

Abstract

Introduction

Conclusions

References

Tables

Figures

⏪

⏩

◀

▶

Back

Close

Full Screen / Esc

Printer-friendly Version

Interactive Discussion



East, edited by: Simmons, M. D., Chapman and Hall, London, 177–219, 1994.

Swart, P. K., Reijmer, J. J. G., and Otto, R.: A re-evaluation of facies on Great Bahama Bank II: variations in the  $\delta^{13}\text{C}$ ,  $\delta^{18}\text{O}$  and mineralogy of surface sediments, *Int. Assoc. Sedimentol. Spec. Publ.*, 41, 47–59, 2009.

5 Tešović, B. C., Glumac, B., and Bucković, D.: Integrated biostratigraphy and carbon isotope stratigraphy of the Lower Cretaceous (Barremian to Albian) Adriatic-Dinaridic carbonate platform deposits in Istria, Croatia, *Cret. Res.*, 32, 301–324, 2011.

Tejada, M. L. G., Suzuki, K., Kuroda, J., Coccioni, R., Mahoney, J. J., Ohkouchi, N., Sakamoto, T., and Tatsumi, Y.: Ontong Java Plateau eruption as a trigger for the early Aptian oceanic anoxic event, *Geology*, 37, 855–858, 2009.

10 Velić, I.: Stratigraphy and palaeobiogeography of Mesozoic benthic foraminifera of the Karst Dinarides (SE Europa), *Geologia Croatica*, 60, 1–113, 2007.

Wagner, P. D.: Geochemical stratigraphy and porosity controls in Cretaceous carbonates near the Oman Mountains, in: *The Geology and Tectonics of the Oman Region*, edited by: Robertson, A. H. F., Searle, M. P., and Ries, A. C., *Geol. Soc. Spec. Publ.*, 49, 127–137, 1990.

15 Weber, J. N. and Woodhead, P. M. J.: Factors affecting the carbon and oxygen isotopic composition of marine carbonate sediments-II. Heron Island, Great Barrier Reef, Australia, *Geochim. Cosmochim. Ac.*, 33, 19–38, 1969.

Weissert, H. and Erba, E.: Volcanism,  $\text{CO}_2$  and paleoclimate: a Late Jurassic-Early Cretaceous oxygen isotope record, *J. Geol. Soc. Lond.*, 161, 695–702, 2004.

20 Wissler, L., Funk, H., and Weissert, H.: Response of Early Cretaceous carbonate platforms to changes in atmospheric carbon dioxide levels, *Palaeogeogr. Palaeocl.*, 200, 187–205, 2003.

Witt, W. and Gökdağ, H.: Orbitolinid biostratigraphy of the Shu'aiba Formation (Aptian), Oman – implications for reservoir development, in: *Micropalaeontology and Hydrocarbon Exploration in the Middle East*, edited by: Simmons, M. D., Chapman and Hall, London, 241–271, 1994.

25

## Bio-chemostratigraphy of the Barremian-Aptian shallow-water

M. Di Lucia et al.

Title Page

Abstract

Introduction

Conclusions

References

Tables

Figures

◀

▶

◀

▶

Back

Close

Full Screen / Esc

Printer-friendly Version

Interactive Discussion



**Table 1.** Lithofacies description and palaeoenvironmental interpretation

Lithofacies associations (LA)	Texture	Skeletal and non-skeletal components	Sedimentary and diagenetic features	Environmental interpretation
Chara-Ostracodal limestones (LA 1)	Mudstone/Wackestone	Thin shelled ostracods (a), characean oogonia (c) and stems (r) small and thin shelled gastropods (r).	Dissolution cavities with vadose silt and/or sparry calcite infilling.	Ephemeral supratidal ponds
Fenestral and/or Microbialitic limestones (LA 2)	Mudstone/Wackestone	Ostracods (c), small miliolids (c), thin-shelled gastropods (r), Thaumatoporella (r).	Fenestrae, birdseyes, dissolution cavities (with vadose silt, sparry calcite or marly infilling), mud-cracks and black pebbles.	Tidal flat and/or very restricted lagoon
Mili-Ostr-Algal limestones (LA 3)	Mudstone/Wackestone	Ostracods (a), small miliolids (a), green algae (c), thin-shelled gastropods (r), textularids (c).	Dissolution cavities with vadose silt and/or sparry calcite infilling.	Intertidal to shallow subtidal protected lagoon
<i>S. dinarica</i> limestones (LA 4)	Wackestone/Packstone	<i>S. dinarica</i> (va), cuneolinids (r), nezzazzatis (r), ostracods (r), peloids (r).	<i>S. dinarica</i> sometimes crushed and isoriented parallel to bedding.	Shallow subtidal protected lagoon
Bio-Peloidal limestones (LA 5)	Packstone/Grainstone	Benthic forams and green algae (a), molluskan shell fragments and ostracods (r). Peloids and intraclasts (a), ooids, oncoids and aggregate grains (r).	Parallel lamination (r), gradation (r).	Shallow subtidal sand bars
For-Algal limestones (LA 6)	Wackestone/Packstone	Benthic forams (a), green algae (c), ostracods (r), molluskan and echinoid shell fragments (c), Lithocodium/Bacinella nodules (c to a) and faecal pellets (r).	Bioturbation.	Subtidal open lagoon
Molluskan limestones (LA 7)	Floatstone	Requienid and/or gastropods (a). Matrix of bio-peloidal-intraclastic wackestone/packstone/ grainstone, with benthic forams (c), green algae (c), Lithocodium/Bacinella (r) and faecal pellets (r).	Bioturbation, Bioerosion of molluskan shells.	Subtidal open lagoon
Palorbitolina limestones and Orbitolinid/codiaceans marls and limestones (LA 8)	Mudstone/Wackestone	Orbitolinids ( <i>P. lenticularis</i> ) (c to a), miliolids and textularids (c), Lithocodium/Bacinella nodules (c), molluskan and echinoid shell fragments (c), sponge spicules (a), oncoids, intraclasts and peloids (r).	Bioturbation, stylonodular structures.	Deep open lagoon
	Packstone	Orbitolinids (va) ( <i>Mesorbitolina. parva</i> , <i>M. texana</i> ) and codiaceans (va) ( <i>B. hochsteteri moncharmontiae</i> ), dasycladaceans (r), textularids (r) and echinoid shell fragments (c), micritic intraclasts (c).	Bioturbation, micritization of orbitolinid shells, stylonodular structures.	

va = very abundant; a = abundant; c = common; r = rare

## Bio-chemostratigraphy of the Barremian-Aptian shallow-water

M. Di Lucia et al.

Title Page

Abstract

Introduction

Conclusions

References

Tables

Figures



Back

Close

Full Screen / Esc

Printer-friendly Version

Interactive Discussion



**Table 2.** Elemental concentration, Sr-isotope ratio and SIS age.

Section	Sample no.	Component	Sr	Mg	Fe	Mn	$^{87}\text{Sr}/^{86}\text{Sr}$	$\pm 2$ s.e. ( $\times 10^{-6}$ )	Age [Ma]				
									Min	Mean	Max		
			[ppm]										
Coccovello	CO 5.8 A-1	rudist	1012	1172	< 0.5	2.3	0.707375						
	CO 5.8 C-4	rudist	929	1036	32.7	3.2	0.707362						
	CO 5.8 B-3	rudist	848	1008	66.5	7.4	0.707382						
						0.707373 (average)	12	122.1	122.9	123.5			
Croce	CR 57.4 A	rudist	1148	1920	94.4	2.4	0.707388						
	CR 57.4 B	rudist	1289	1702	4.0	0.8	0.707429						
	CR 57.4 C	rudist	1411	1967	110.5	0.0	0.707393						
						0.707403 (average)	26	122.9	124.1	125.2			

Numerical age from McArthur et al. (2001, look-up table version 4: 08/04) calculated by combining the statistical uncertainty of the mean of the isotopic values with the uncertainty of the seawater curve.

**Table 3.** Statistical results for C and O isotopes covariation in the studied sections.

Section	LA	n	r	a	b
Croce	LA1	2	*	*	*
	LA2	17	0.74	0.22	0.8
	LA3	14	0.78	0.41	-1.22
	LA4	2	*	*	*
	LA5	73	0.31	0.14	-0.83
	LA6	22	0.52	0.48	-1.97
	LA7	3	*	*	*
	LA8	17	0.21	0.22	-2.24
	ALL	150	0.30	0.18	-1.11
Motola	LA1	5	0.93	0.86	-2.07
	LA2	27	0.33	0.28	-2.36
	LA3	22	0.29	-0.26	-1.98
	LA4	2	*	*	*
	LA5	49	0.6	0.5	-3.11
	LA6	12	0.5	0.44	-3.07
	LA7	7	0.35	0.13	-2.1
	LA8	13	0.34	0.36	-2.93
	ALL	137	0.30	0.26	-2.6
Coccovello	LA1	7	0.59	-0.17	-2.27
	LA2	54	0.25	0.1	-2.15
	LA3	15	0.08	0.04	-2.28
	LA4	1	*	*	*
	LA5	38	0.43	0.11	-2.35
	LA6	3	*	*	*
	LA7	2	*	*	*
	LA8	9	0.05	0.03	-2.64
	ALL	129	0.18	0.06	-2.3

LA = lithofacies association; n = number of observations; r = Pearson correlation coefficient; a = slope of the regression line; b = intercept of the regression line; \* = not calculated when  $n < 5$

**Bio-chemostratigraphy of the Barremian-Aptian shallow-water**

M. Di Lucia et al.

Age	Apenninic carbonate platform		Adriatic carbonate platform		N-Israel carbonate platform
Albian (12 My)	<i>Peneroplis parvus</i> taxon-range zone (upper boundary: earliest Cenomanian)	<i>Ostracoda/Miliolidae</i> assemblage zone (upper boundary: middle Cenomanian)	<i>V. dercourti</i> taxon-range zone	<i>N.convexa</i> taxon-range zone	
	<i>Sabaudia minuta</i> interval zone	<i>Dictyoconus algerianus</i> taxon-range zone	<i>M.texana/V. dercourti</i> interval zone	<i>V. dercourti</i> partial-range zone	
Aptian (13 My)	<i>Salpingoporella dinarica</i> taxon-range zone	<i>Archaeoalveol. reichelti</i> taxon-range zone	<i>Salpingoporella dinarica</i> Abundance zone	<i>Mesorbitolina subconvexa</i> taxon-range zone	
		<i>Salpingoporella dinarica</i> taxon-range zone	<i>Bacinella irregularis</i> assemblage zone	<i>Mesorbitolina parva</i> lineage zone	<i>M. texana/M. parva</i> interval zone
			<i>?Cuneolina scarsellai/ Cuneolina camosauri</i> assemblage zone	<i>Salpingoporella melitae/ Salpingoporella muhelbergii</i> interval zone	<i>Palorbitolina lenticularis</i> superzone
<i>Palorbitolina lenticularis</i> superzone	<i>C. capuensis-P. lenticularis</i> interval zone	<i>Mesorb. lotzei</i> lineage zone			<i>P. cornyi/M. lotzei</i> interval zone
		<i>P. wienandsi</i> lineage zone	<i>P. lenticularis-C. decipiens</i> interval zone		
Barremian (5 My)	<i>Campanellula capuensis</i> taxon-range zone	<i>?Cuneolina scarsellai/ Cuneolina camosauri</i> assemblage zone	<i>Clypeina? solkani</i> Abundance zone	<i>P. cornyi</i> lineage zone	
				<i>R. giganteus/P. lenticularis</i> assemblage zone	
Hauterivian (6.4 My)	<i>Cuneolina laurentii</i> interval zone (lower boundary: latest Valanginian)	<i>?Cuneolina scarsellai/ Cuneolina camosauri</i> assemblage zone	<i>Clypeina? solkani</i> Abundance zone	<i>C. capuensis</i> taxon-range zone	
				<i>V. camosauri-C. capuensis</i> interval zone	
	De Castro (1991)	Chiocchini et al. (2008)	Husinec and Sokač (2006)	Velić (2007)	Bachmann and Hirsch (2006)

**Fig. 1.** Barremian–Aptian biostratigraphy of central-southern Tethyan carbonate platforms. These schemes suffer of low resolution and poorly constrained chronostratigraphic calibration.

Title Page

Abstract

Introduction

Conclusions

References

Tables

Figures



Back

Close

Full Screen / Esc

Printer-friendly Version

Interactive Discussion

## Bio- chemostratigraphy of the Barremian-Aptian shallow-water

M. Di Lucia et al.

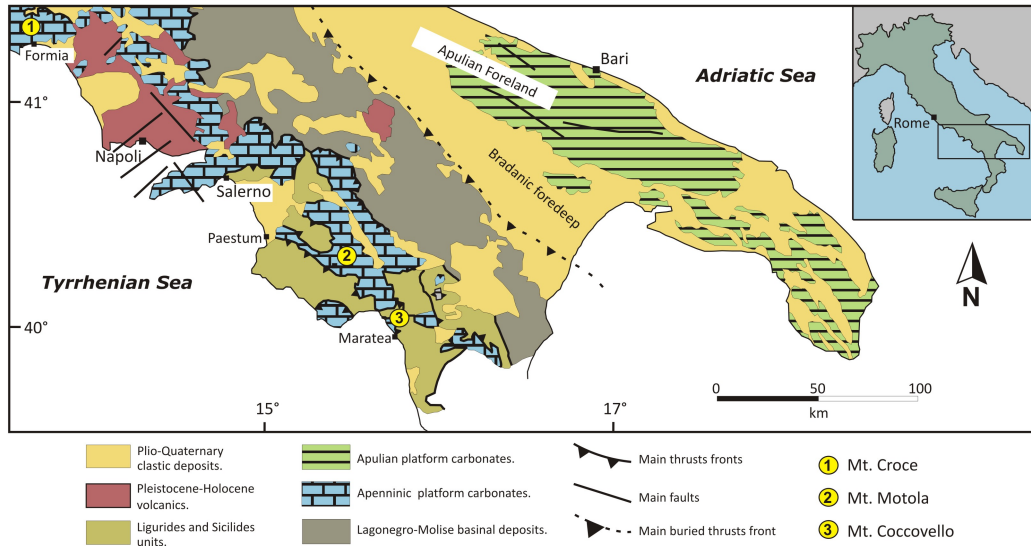


**Fig. 2.** Schematic geological map of the central-southern Apennines, with location of the studied sections (modified from Bonardi et al., 1988).

Title Page

Abstract

Introduction

Conclusions

References

Tables

Figures



Back

Close

Full Screen / Esc

Printer-friendly Version

Interactive Discussion

**Bio-  
chemostratigraphy of  
the Barremian-Aptian  
shallow-water**

M. Di Lucia et al.

Title Page

Abstract

Introduction

Conclusions

References

Tables

Figures

◀

▶

◀

▶

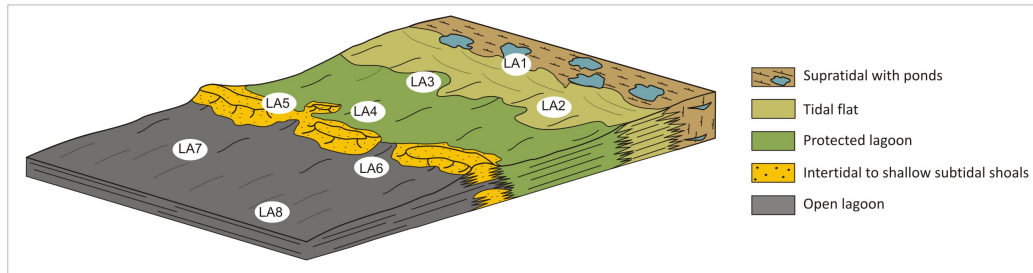
Back

Close

Full Screen / Esc

Printer-friendly Version

Interactive Discussion

**Fig. 3.** Schematic depositional model with facies distribution.

## Bio-chemostratigraphy of the Barremian-Aptian shallow-water

M. Di Lucia et al.

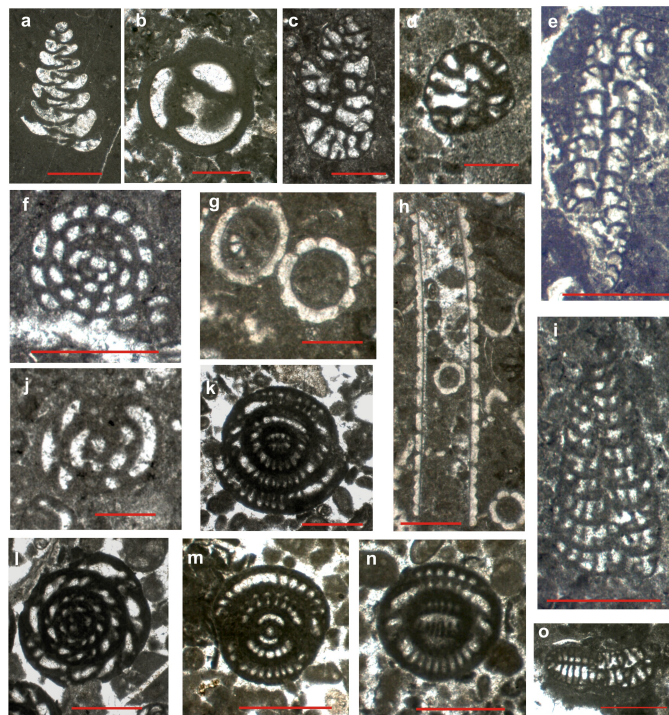


**Fig. 4.** (a) *Praechrysalidina infracretacea*, axial section (Mt. Croce, sample CR 70.5); (b) *Praechrysalidina infracretacea*, transversal section (Mt. Croce, CR 55.4); (c) *Voloshinoides murgensis*, sub-axial section (Mt. Coccovello, CO 1,8); (d) *Voloshinoides murgensis*, sub-transversal section (Mt. Motola, MO 89.7); (e) *Cuneolina parva*, axial section (Mt. Motola, MO 137,7); (f) *Debarina hahounerensis*, equatorial section (Mt. Coccovello, CV 79.2a); (g) *Salpingoporella dinarica*, transversal section (Mt. Motola, MO 103,8); (h) *Salpingoporella dinarica*, axial section (Mt. Motola, MO 103,8); (i) *Cuneolina parva*, axial section (Mt. Motola, MO 137.7); (j) *Debarina hahounerensis*, sub-axial section (Mt. Coccovello, CV 79.2a); (k) *Archaeoalveolina reicheli*, sub-axial section (Mt. Coccovello, CO 30.2); (l) *Archaeoalveolina reicheli*, equatorial section (Mt. Coccovello, CO 30.2); (m) *Archaeoalveolina reicheli*, axial section (Mt. Coccovello, CO 30.2); (n) *Archaeoalveolina reicheli*, tangential section (Mt. Coccovello, CO 30.2); (o) *Cuneolina parva*, sub-transversal section (Mt. Motola, MO 137,7). Scale bar is 500 microns for all photographs.

Title Page

Abstract

Introduction

Conclusions

References

Tables

Figures

◀

▶

◀

▶

Back

Close

Full Screen / Esc

Printer-friendly Version

Interactive Discussion

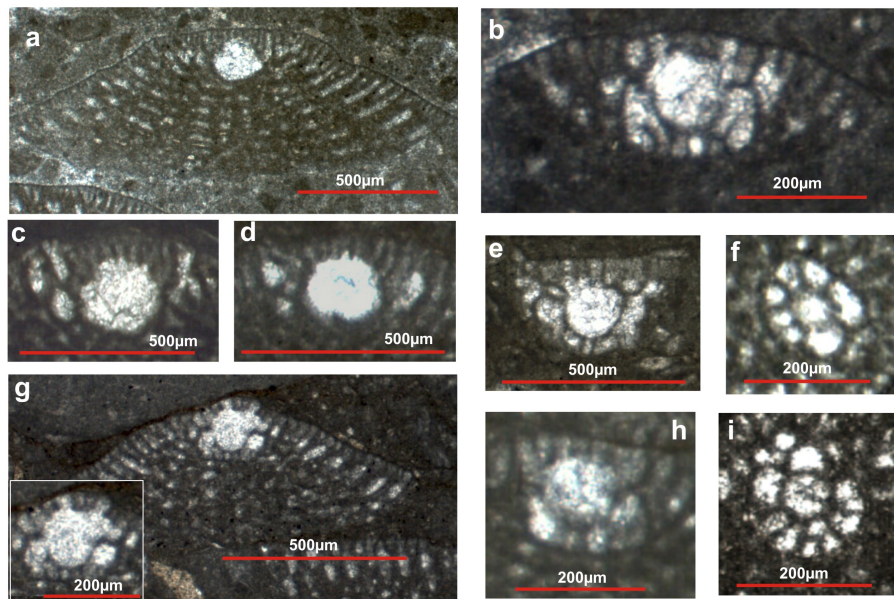


**Fig. 5.** (a) *Palorbitolina lenticularis*, axial sections through the embryonic apparatus (Mt. Coccovello, sample CV 71.7); (b) *Mesorbitolina texana*, axial section through the embryonic apparatus; (c–d) *Palorbitolina lenticularis*, axial section through the embryonic apparatus (Mt. Coccovello, CV 65.4a); (e) *Mesorbitolina texana*, axial section through the embryonic apparatus (Mt. Coccovello, CV 77,9a); (f) *Mesorbitolina texana*, subtransversal section of the embryonic apparatus, slightly oblique through the subembryonic zone (Mt. Coccovello, CV 77,9a); (g) *Mesorbitolina parva*, axial section through the embryonic apparatus, with detail of the embryonic apparatus (Mt. Coccovello, CV 77,9a); (h) *Mesorbitolina parva*, axial section through the embryonic apparatus (Mt. Coccovello, CV 77,9a); (i) *Mesorbitolina parva*, subtransversal section of the embryonic apparatus, oblique through the subembryonic zone (Mt. Coccovello, CV 77,9a).

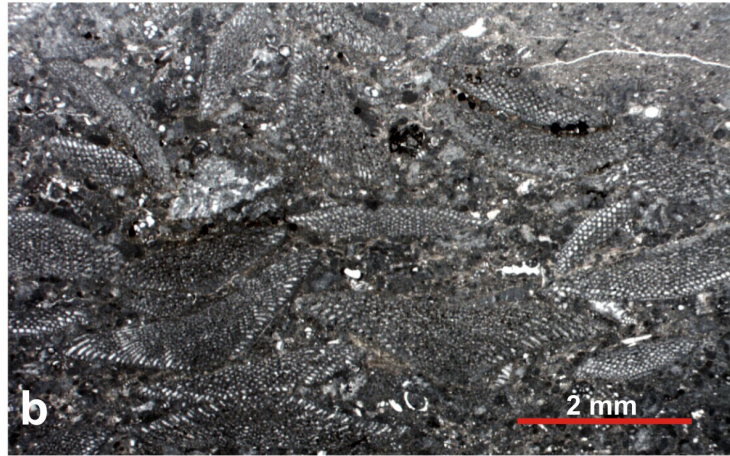


**Fig. 6.** Marly interval of the “Orbitolina level” at Mt. Croce: **(a)** outcrop, **(b)** microfacies (sample CR 75.9).

## SED

3, 789–838, 2011

### Bio- chemostratigraphy of the Barremian-Aptian shallow-water

M. Di Lucia et al.

Title Page

Abstract

Introduction

Conclusions

References

Tables

Figures

◀

▶

◀

▶

Back

Close

Full Screen / Esc

Printer-friendly Version

Interactive Discussion



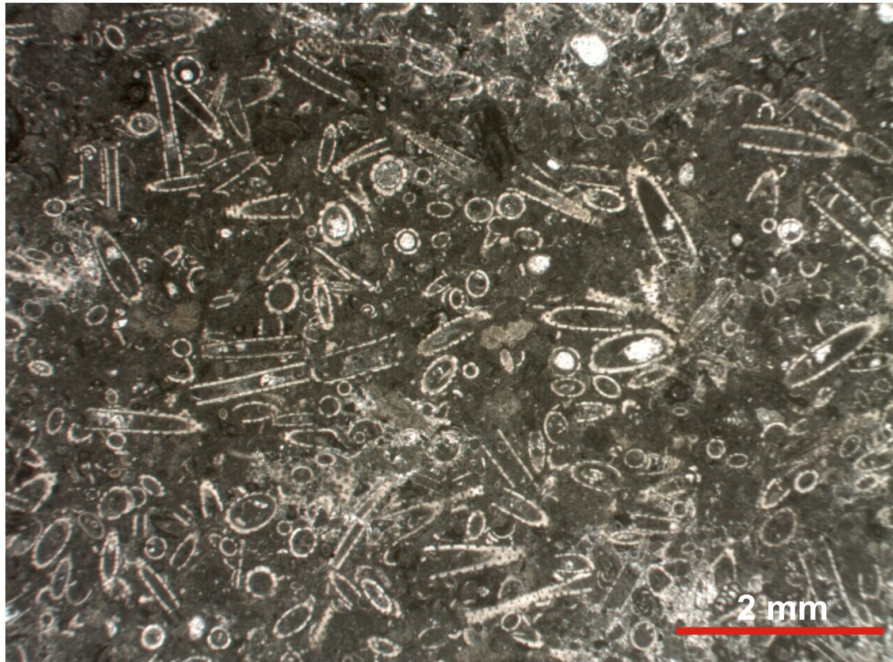


**Fig. 7.** *Salpingoporella dinarica* acme at Mt. Motola, microfacies (sample MO 103.8).

## SED

3, 789–838, 2011

### Bio- chemostratigraphy of the Barremian-Aptian shallow-water

M. Di Lucia et al.

Title Page

Abstract

Introduction

Conclusions

References

Tables

Figures

◀

▶

◀

▶

Back

Close

Full Screen / Esc

Printer-friendly Version

Interactive Discussion



## Bio-chemostratigraphy of the Barremian-Aptian shallow-water

M. Di Lucia et al.

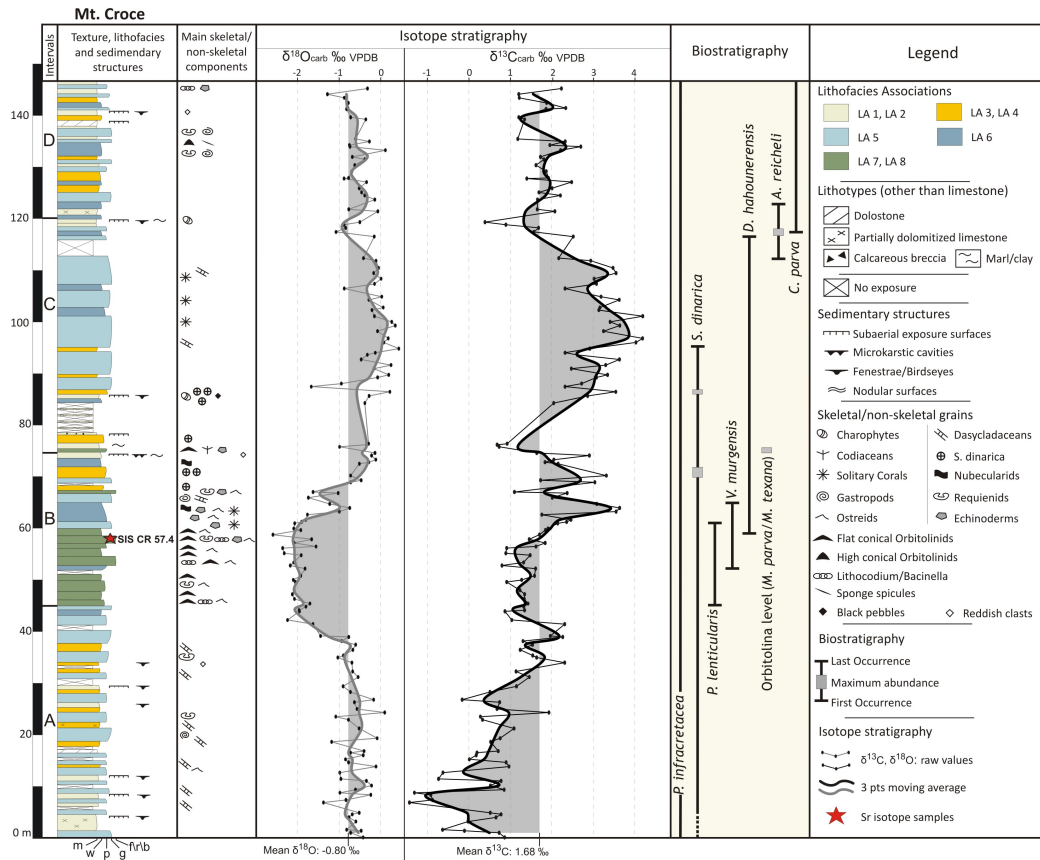


**Fig. 8.** Mt. Croce section: lithological–sedimentological log, isotope stratigraphy and biostratigraphy. The thick curves represent the 3-point moving averages of O- (grey) and C-isotope ratios (black).

Bio-  
chemostratigraphy of  
the Barremian-Aptian  
shallow-water

M. Di Lucia et al.

Title Page

Abstract

Introduction

Conclusions

References

Tables

Figures



Back

Close

Full Screen / Esc

Printer-friendly Version

Interactive Discussion

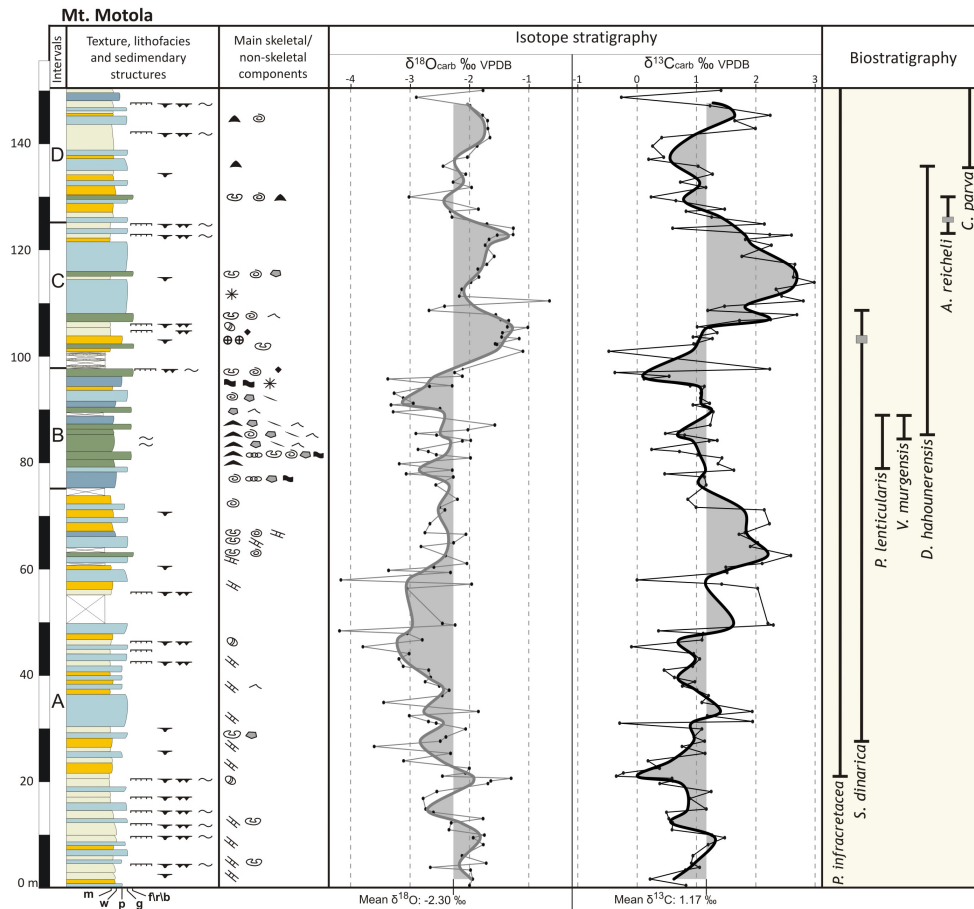


**Fig. 9.** Mt. Motola section: lithological–sedimentological log, isotope stratigraphy and biostratigraphy. The thick curves represent the 3-point moving averages of O- (grey) and C-isotope ratios (black). See Fig. 6 for a key to colors, patterns and symbols.

## Bio-chemostratigraphy of the Barremian-Aptian shallow-water

M. Di Lucia et al.

Title Page

Abstract

Introduction

Conclusions

References

Tables

Figures

◀

▶

◀

▶

Back

Close

Full Screen / Esc

Printer-friendly Version

Interactive Discussion

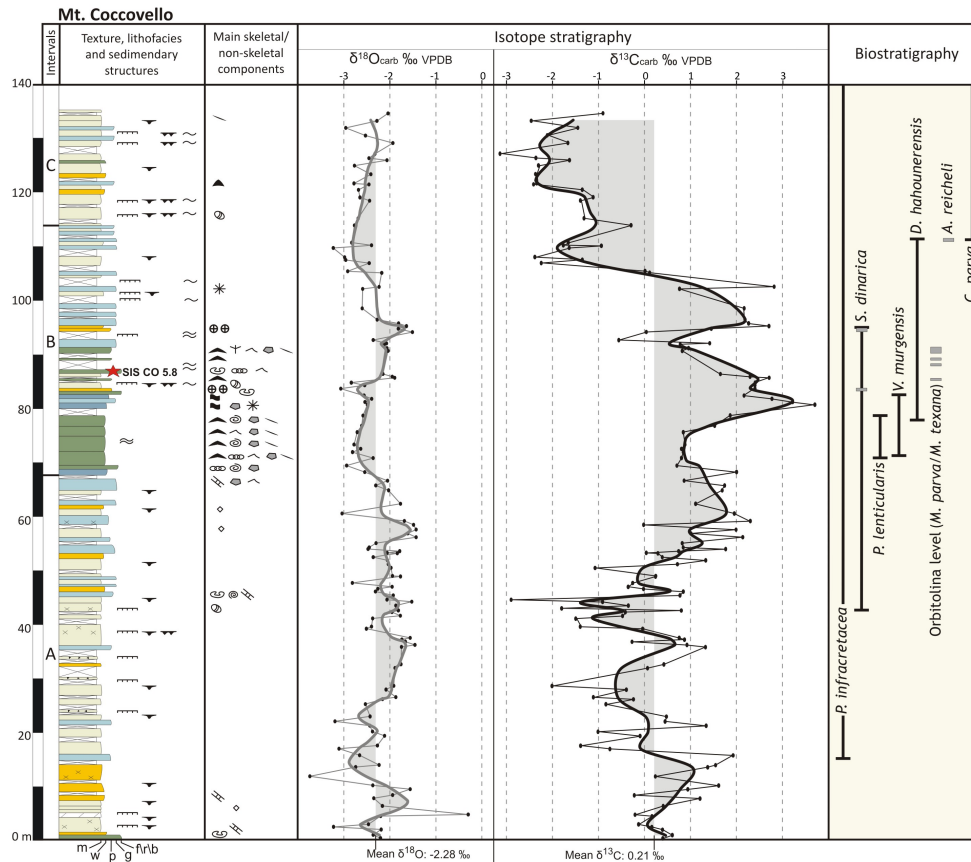


**Fig. 10.** Mt. Coccovello section: lithological–sedimentological log, isotope stratigraphy and biostratigraphy. The thick curves represent the 3-point moving averages of O- (grey) and C- isotope ratios (black). See Fig. 6 for a key to colors, patterns and symbols.

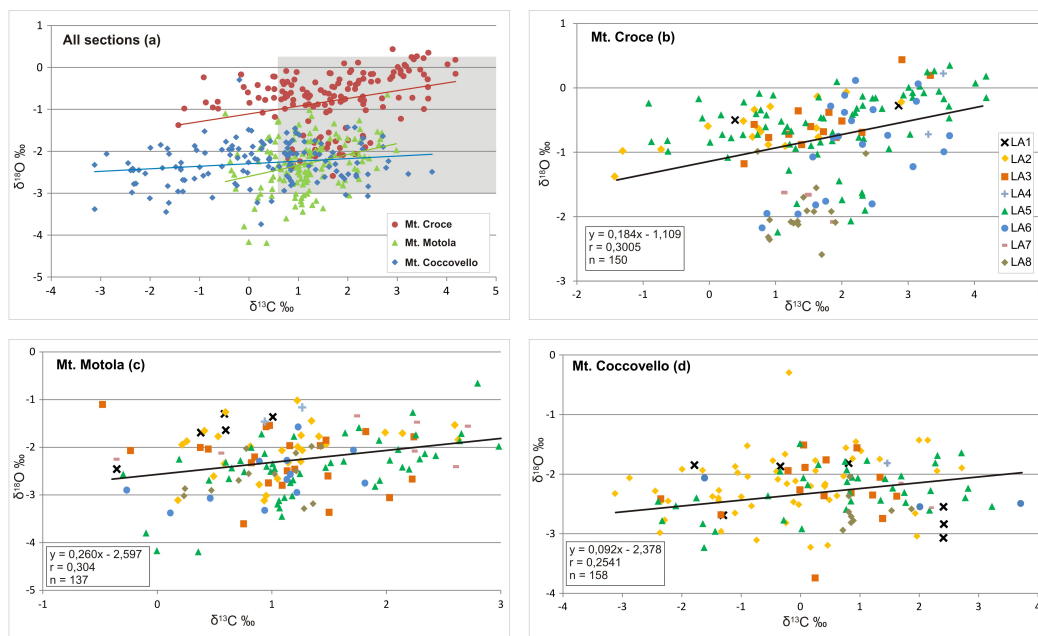


**Fig. 11.** Cross-plots of  $\delta^{13}\text{C}$  vs.  $\delta^{18}\text{O}$  for the whole dataset (**a**) and for each studied section (**b–d**). The all-lithofacies dataset (**a**) shows very low to moderate covariance ( $r = 0.18 - 0.30$ ). Supratidal and intertidal lithofacies associations show higher covariance of stable isotope ratios (diagrams b–c; see also Table 3). On the other hand, there is no clear relation between lithofacies and isotopic value. The shaded quadrangle in diagram (**a**) indicates the range of well-preserved biotic calcite of shallow marine tropical-subtropical carbonates (from Prokoph et al., 2008).

Title Page

Abstract

Introduction

Conclusions

References

Tables

Figures

◀

▶

◀

▶

Back

Close

Full Screen / Esc

Printer-friendly Version

Interactive Discussion

## Bio-chemostratigraphy of the Barremian-Aptian shallow-water

M. Di Lucia et al.

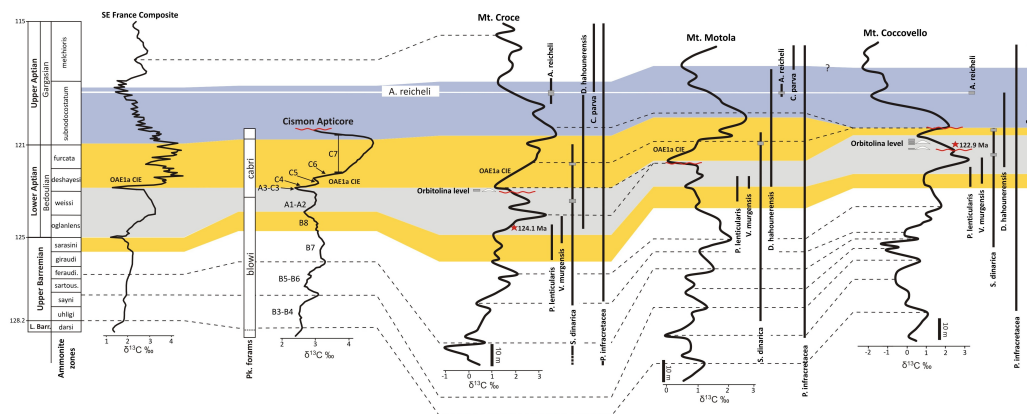


**Fig. 12.** Chemostratigraphic correlation of the three sections of the Apenninic carbonate platform with the reference section of the Cison Apticore (Belluno Basin, northern Italy) (Erba et al., 1999) and with the composite hemipelagic curve of southeastern France (Föllmi et al., 2006 and references therein). This correlation uses as independent tie-points a Gargasian age for *A. reicheli* (see text) and the numerical ages of two levels dated by strontium isotope stratigraphy. The nomenclature of chemostratigraphic segments is from Wissler et al. (2003; B3–B8/A1–A3) and from Menegatti et al. (1998; C3–C7). The ammonite and planktonic foraminiferal biozones and their calibration to the Geological Time Scale are from Gradstein et al. (2004).

Title Page

Abstract

Introduction

Conclusions

References

Tables

Figures

◀

▶

◀

▶

Back

Close

Full Screen / Esc

Printer-friendly Version

Interactive Discussion

## Bio- chemostratigraphy of the Barremian-Aptian shallow-water

M. Di Lucia et al.

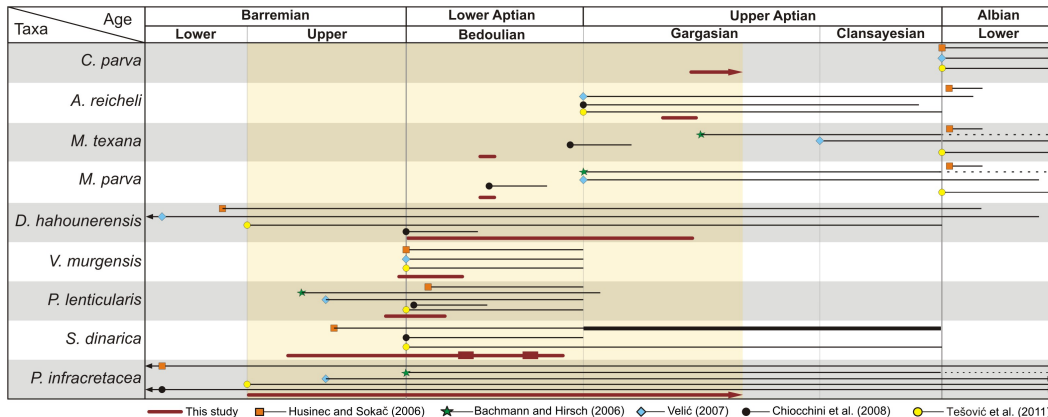


**Fig. 13.** Chronostratigraphic calibration of the Apenninic carbonate platform biostratigraphy. The calibration is based on the chemostratigraphic correlation with well-dated basinal sections (see Fig. 10). The chronostratigraphic calibration of the same biostratigraphic events, proposed by previous works on the Apenninic and other central and southern Tethyan carbonate platforms, is given for comparison. See the text for a discussion. The shaded field indicates the chronostratigraphic interval covered by the sections studied in this paper.

Title Page

Abstract

Introduction

Conclusions

References

Tables

Figures

◀

▶

◀

▶

Back

Close

Full Screen / Esc

Printer-friendly Version

Interactive Discussion